New cellular ceramics from high alkane phase emulsified suspensions (HAPES)

Suelen Barg *, Elisângela Guzi de Moraes, Dietmar Koch, Georg Grathwohl

Ceramic Materials and Components, University of Bremen, D-28359 Bremen, Germany

1. Introduction

High performance ceramics with controlled open porosity find their applications in many different fields of modern technologies especially where fluid and gas transport through the microstructure is required. These include filtration of molten metals and hot gases, catalytic carriers, support for batteries and fuel cells, electrodes, bioreactors, radiant burners, scaffolds for bone replacement and many others.[1–4] While porous ceramics are characterized by several advantageous properties, the microstructural features, in particular the porosity parameters are of crucial importance for their successful application.

The fabrication of porous ceramics makes use of different principles and processes, and excellent recent reviews are available on this subject.[2,3] Besides more conventional techniques[5,6] a direct foaming method has been developed where an alkane phase is emulsified in an aqueous ceramic powder suspension.[7,8] Emulsions and wet foams are used in a broad range of technological applications especially in cosmetic and food technologies.[9] Furthermore, emulsions can be used as templates for the determination of the porosity parameters in inorganic porous structures. In the case of surfactant stabilized emulsions, the structure is normally set via sol–gel processes what requires controlled chemical reactions, consumes time and cannot be easily applied to different compositions.[10] The use of particles for the long-term stabilization of emulsions can be applied to produce porous ceramics of different compositions without the necessity of chemical reactions for the consolidation of emulsions.[11,12]

In the processing route presented here surfactant stabilized emulsions are employed as efficient intermediates for the determination of the porosity parameters during direct foaming. This versatile technique can be adapted for many different compositions and systems, providing a combination of important advantages in particular the tailored microstructural features and highly interconnected cells associated with excellent mechanical properties.

In emulsification processes an immiscible fluid is dispersed in another fluid by rupturing large droplets into smaller ones aided by applied shear flow and a surface-active agent. Surfactants can be used as emulsifiers in the preparation of emulsions and as stabilizers in the production of foams.[13,14] In contrast

* Corresponding author.
E-mail address: sbarg@uni-bremen.de (S. Barg).

to the dynamic adsorption and desorption of surfactants, colloidal particles can serve as stabilizers due to their irreversible adsorption at gas–liquid interfaces resulting in ultra-stable wet foams.[2,12,15]

The theoretical understanding of the emulsification process is fairly limited to the rupturing of an isolated droplet first proposed by Taylor in the 1930s.[16] According to Taylor's model, where an isolated, spherical droplet of radius R_0 with a relatively low viscosity η_d is dispersed in a fluid of viscosity η_c, the droplets will deform into an ellipsoid or elongated cylinder. Normally the rupture of these elongated cylinders in smaller droplets is achieved by the so-called Rayleigh instability reducing the high interfacial energy due to the elongated droplets. Deformation of the dispersed phase only takes place when the shear stress $\eta_c\dot{\gamma}$ surpasses the interfacial stress σ/R_0, where $\dot{\gamma}$ is the shear rate and σ is the interfacial tension. The ratio between these two stresses is defined as the capillary number (Ca). When the capillary number exceeds a critical value, Ca_{crit}, the elongated droplet will rupture into smaller droplets of average radius R according to Eq. (1). Ca_{crit} depends on the viscosity ratio between dispersed and continuous phase (η_d/η_c) and the type of flow[16–21]:

$$R \propto \mathrm{Ca}_{\mathrm{crit}} \frac{\sigma}{\eta_c \dot{\gamma}} \tag{1}$$

This model has also been applied for the prediction of bubble size as a function of suspension composition in particle-stabilized emulsions.[17] A similar analysis is taken in this work for surfactant stabilized emulsions, to evidence the influence of the shear rate on the final droplets size.

In contrast to dilute emulsions with low amounts of dispersed phase, in concentrated emulsions the droplets are close together and therefore the interaction between them plays a very important role in the emulsion properties. For this reason, rheological properties and the degree of stability of these emulsions would be significantly different from emulsions with low amounts of dispersed phase. Consequently, in concentrated emulsions the droplet size of the dispersed phase will attract particular attention due to its strong influence on the rheological properties and stability of the emulsion.[9,21,22]

New mechanically stable ceramic foams with open porosity are developed in this work by a simple direct foaming process in which a highly concentrated alkane phase is emulsified in a stabilized aqueous powder suspension. Here the emulsified suspensions are consolidated by the expansion of the alkane droplets due to foaming and drying of the aqueous solvent. In contrast to the recently developed direct foaming process where foaming is accompanied by a high expansion due to evaporation of the alkane phase,[7] the high concentration of alkane droplets restricts their mobility and modifies the rheological properties leading to a reduced expansion during foaming.

Consequently, the high alkane phase emulsified suspensions (HAPES), in particular the droplet size, can be mainly controlled by the stresses applied in their surface during the stirring process. This foaming process provides then a high flexibility in the production of porous ceramic parts with the advantages of highly interconnected cells and controllable porosity parameters. While in this paper alumina foams are produced, this technique may also be applied to other oxide and non-oxide ceramics, light and even heavy metals depending on the adjustment of dispersion agents and surfactants for the different powder surface chemistries.

The control of the droplet size distribution is of extreme importance in the development of the ceramic foams as it determines the rheological properties of the HAPES as well as the stereological parameters of the final microstructures. It is then the objective of this work to investigate the influences of the suspension particle content as well as the mechanical stirring velocity with respect to droplet size distribution and viscosity of the final emulsified suspensions. The dominating factors and relationships will be evaluated and the processes responsible for the droplet formation and fragmentation as represented in Eq. (1) shall be described. Thus, the control of the investigated parameters should result in designable HAPES and consequently controlled ceramic foam microstructures.

2. Materials and methods

2.1. Materials

Powder suspensions were prepared using deionised water and α-Al_2O_3 powder (Alcoa CT 3000 SG) with an average particle diameter (d_{50}) of 500 nm and a specific surface area of 7.5 m^2/g. A low molecular weight (320 g/mol) polyacrylic acid commercially available as Dolapix CE-64 (Zschimmer & Schwarz) was added as negatively charged electrosteric dispersion agent to stabilize the suspensions. The anionic surfactant sodium lauryl sulphate (SLS) (BASF, Lutensid AS 2230) was used for the production of the emulsions. The addition of this surfactant had to take into account the zeta potential and isoelectric point (IEP) of the alumina suspension. Therefore it was used under alkaline conditions (pH 9.5) where the strong negative zeta potential was provided by the dispersion agent.[7] Decane ($C_{10}H_{22}$) from Fluka was used as dispersed phase.

2.2. Preparation of HAPES

For the production of the HAPES the first step is the preparation of a stabilized alumina powder suspension. This step is followed by the formation of an emulsion as uniform dispersion of a high concentrated alkane phase (70 vol.% in this case) in the alumina suspension. For this purpose the anionic surfactant as stabilizer and the alkane phase are added after the stabilized alumina suspension is prepared.

The stabilized powder suspensions were prepared as follows: dry alumina powder was slowly added to deionised water containing Dolapix CE–64 (0.74 wt% related to alumina) as dispersion agent under severe mixing. Dispersion and homogenization was carried out in a laboratory mixer (Dispermat LC, VMA Getzmann GmbH) with a 30-mm dispersing tool operating at a mixing velocity of 2500 rpm for 20 min. In former experiments[8] the optimal powder dispersion was investigated and attributed to the efficiency of this procedure applying the electrosteric dispersion agent. The particle content in the suspensions was set to 15, 30 and 45 vol.%. Afterwards the suspensions

were subjected to de-aeration to remove undesired entrapped bubbles. This procedure was performed in a container under reduced pressure (5 kPa).

Emulsified suspensions were prepared by adding 70 vol.% decane and 0.33 vol.% anionic surfactant to the ceramic suspensions containing different particle contents under further mechanical stirring for 2.5 min at different stirring velocities (from 600 to 4000 rpm). The suspensions were emulsified under reduced pressure at room temperature to avoid the abundant incorporation of air bubbles. A moderately reduced pressure of 10 kPa was chosen with respect to the evaporation of decane which has a vapor pressure of 4.6 kPa at 20 °C.

2.3. Characterization methods for HAPES

The microstructure, in particular the droplet size distribution of the HAPES was analysed by the use of a fluorescence microscope in the reflected mode combined to a digital camera. Immediately after mechanical stirring the HAPES samples were transferred into closed quartz cells (Hellma) to avoid changes in the system. The alkane phase was dyed with Pyrene (Fluka), making the alkane droplets fluorescent at an emission wavelength λ_{Em} of 375 nm. With this technique it was possible to distinguish the alkane droplets from the alumina suspension. For each condition two pictures were taken and a minimum of 140 droplets were individually measured for statistical analysis with the use of Axio Vision LE image analysis program. The average droplet size d_{50} was determined from the cumulative droplet size distribution curve corresponding to the droplet diameter at a cumulative droplet percentage of 50% (number distribution), while d_{10}, and d_{90} represent the droplets diameters at 10% and 90% of the cumulative distribution.

HAPES flow curves were analysed with a shear-controlled rheometer (Model 88 BV, Bohlin Reologi, UK Ltd.) with a cone-plate measurement system. The experiments were realized using an increasing shear rate, i.e., from 0.08 to 500 s^{-1} within 3 min. The temperature was kept at 25 °C during the measurements.

2.4. Foaming, drying and sintering

The HAPES were poured into polymeric molds keeping the upper surface opened to the atmosphere. Further limited foaming proceeded as a consequence of the evaporation of the alkane phase accompanied by minimal expansion of the bubbles. The drying of the foams was realized at room temperature during 4 days.

After the consolidation, the shaped green alumina foams were sintered at 1550 °C for 2 h with heating and cooling rates of 2 and 3 K/min, respectively.

2.5. Characterization of the sintered foams

The microstructure of the sintered ceramic foams was analysed from micrographs taken by scanning electron microscopy (SEM) (Camscan 24). Cell sizes were individually measured in planar sections with the help of an image analysis program (AnalySIS). The average cell size d_{50}, d_{10} and d_{90} were determined from the cumulative cell size distribution curve. The volumetric density ρ_v of the foams was determined from the mass and dimensions of the sintered bodies. The porosity P was

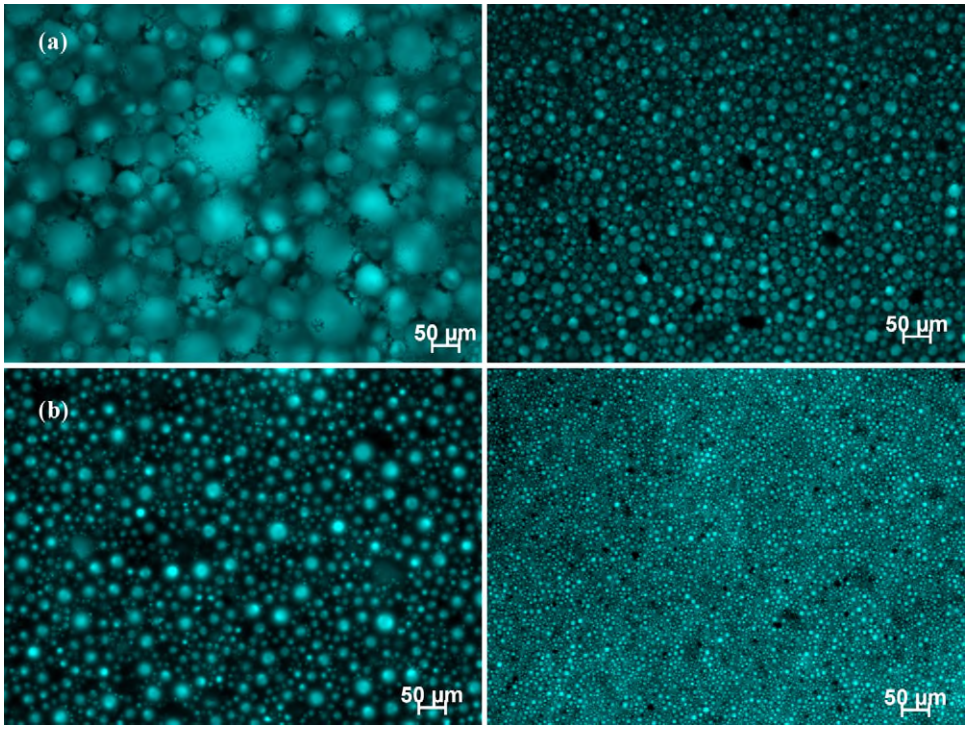

Fig. 1. Typical microstructures of HAPEs containing 70 vol.% decane and 0.33 vol.% surfactant. (a) 15 vol.% and (b) 45 vol.% particle content suspensions. Emulsification proceeded under a stirring velocity of 600 rpm (left) and 2000 rpm (right).

then calculated as $P = 1 - \rho_v/\rho_t$ with ρ_t (3.9 g/cm^3) corresponding to the theoretical density of alumina.

3. Results and discussion

3.1. Influence of mechanical stirring velocity and suspension particle content

The HAPES in closed quartz cells were analysed immediately after mechanical stirring under fluorescence microscopy. Typical microstructures are shown in Fig. 1 where the alkane droplets are uniformly distributed in the ceramic suspension. With the increase in the suspensions particle content the alkane average droplet size decreases for all emulsification stirring velocities. When the stirring velocity is increased, an improved homogeneity of the droplet size distribution is observed and the average droplet size is strongly reduced.

The quantitative results of the droplet size distribution are presented in Fig. 2. It is shown that the broad distribution of rather large droplet sizes obtained by the slow stirring rate and low particle content is strongly reduced by both, i.e., by increasing the particle content and the stirring rate. While the droplet size distribution in slowly stirred HAPES with high particle content shows some broadness a strong size reduction with a very close distribution is reached at the high stirring rate. It is also to be noticed that the reduction of the average droplet size with the increase of the stirring velocity is more abrupt for HAPES containing lower particle content suspensions than in the case of higher concentrated ones (Fig. 3). This reflects the fact that the larger the droplets the higher is the rate of fragmentation while for smaller droplets the decrease is much lower approaching a saturation diameter.[10,11]

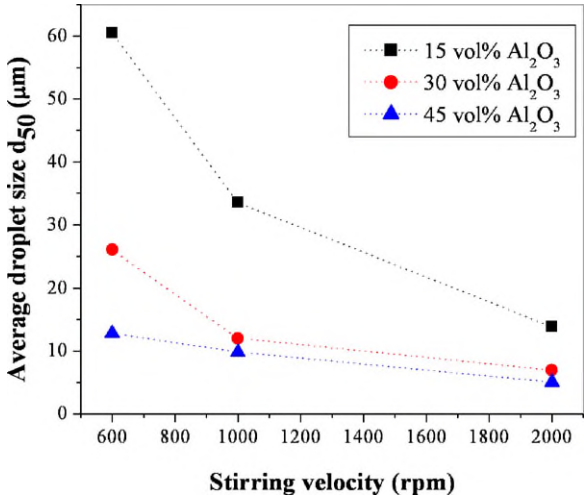

Fig. 3. Effect of emulsification stirring velocity and suspension particle content on the average droplet size (d_{50}) of HAPES.

By rising the stirring rate from 600 to 2000 rpm, reduction of the average droplet size from 60 to 14 and from 13 to 5 μm

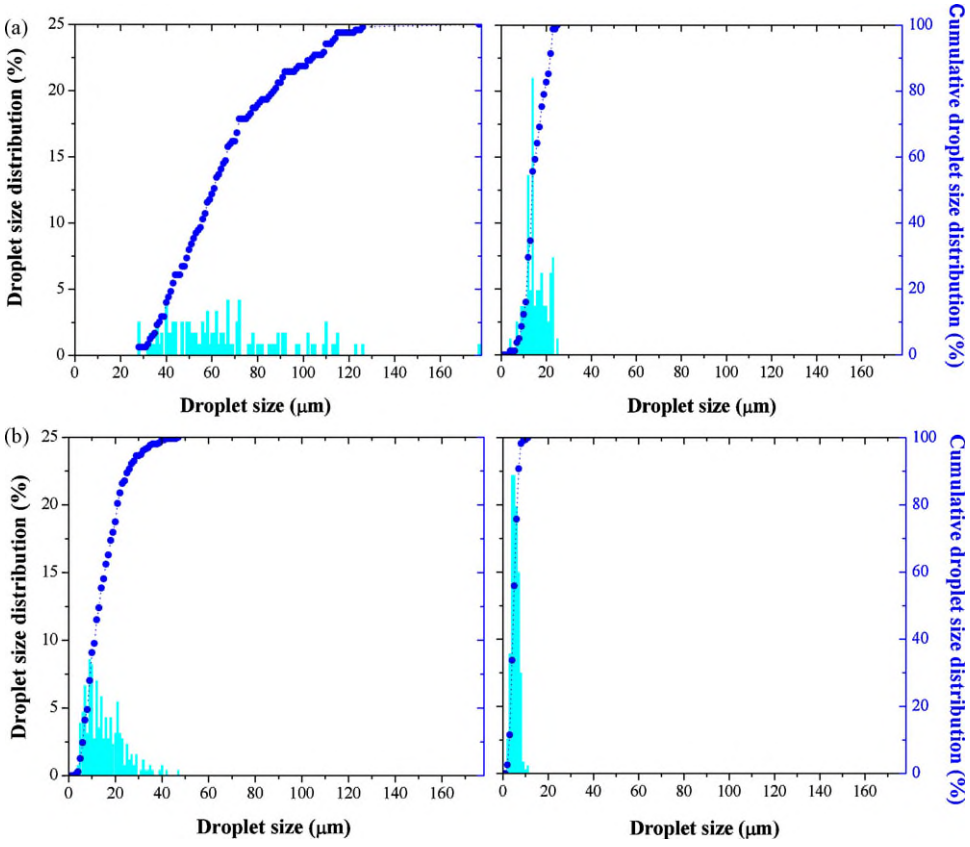

Fig. 2. Effect of emulsification stirring velocity and particle content on droplet size distributions of HAPES containing 70 vol.% decane and 0.33 vol.% surfactant. (a) 15 vol.% and (b) 45 vol.% particle content suspensions emulsified under 600 rpm (left) and 2000 rpm (right).

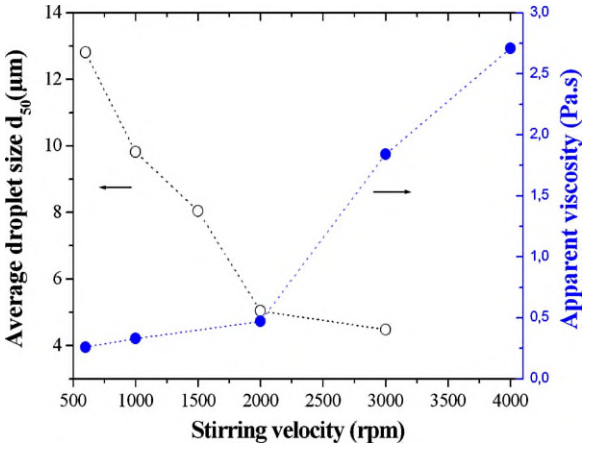

Fig. 4. Effect of mechanical stirring on the droplet size and viscosity of HAPES with 45 vol.% particle content.

is observed for HAPES containing 15 and 45 vol.% particles, respectively.

It is remarkable that very small droplets in close distribution are achieved for the case of high stirring velocity and also high particle contents although a non-homogeneous shear rate (in this case via Dispermat LC mixer) was applied in the HAPES emulsification process. This effect can be recognised in the extreme cases where HAPES containing 15 vol.% particles emulsified under 600 rpm provides droplet sizes of 37 and 104 µm, for d_{10} and d_{90}, respectively, while 45 vol.% suspensions emulsified at 2000 rpm turn out as very narrow droplet size distribution of 3 and 7 µm for d_{10} and d_{90}, respectively (Fig. 2).

The smaller the droplet size, the higher is the droplet concentration in the system and consequently the higher is the restriction to their mobility. In order to investigate this effect of the droplet size on the rheological behaviour and stability of the system, rheological and microstructural investigations were undertaken in HAPES with 45 vol.% particle suspensions emulsified under increasing stirring velocities up to a maximum of 4000 rpm (Fig. 4).

The average droplet size of HAPES with 45 vol.% solid particles is rather small and decreases at higher stirring rates. In Fig. 4 the effect of the further enhanced stirring rates beyond 2000 rpm is shown; the average droplet size hardly decreases anymore due to the resistance in the distortion of smaller droplets. The droplets size distribution resulting from HAPES emulsified under 4000 rpm could not be identified by fluorescence microscopy.

The rheological measurements of HAPES revealed shear thinning flow curves. This aspect may in part be due to the presence of agglomerates in the ceramic suspension that during shearing are deformed and eventually disrupted, resulting in a reduction of the viscosity. If the shear rate applied in the emulsions during the rheological experiments is higher than applied during the previous emulsification process the fragmentation of the droplets can continue. Therefore, the viscosity of the emulsified suspensions was analysed at a low shear rate ($113\,s^{-1}$), to ensure that no droplet rupture had taken place. The increase in stirring rate leads to smaller droplets of higher concentration resulting in an increase of the apparent viscosity. When emulsification is realized under 3000 rpm the high concentration of small droplets leads to a significant increase of the apparent viscosity.

The results show that the droplet size distribution is influenced by the particle content of the suspensions and the emulsification stirring velocity. High particle contents and the increase of the stirring velocity decrease the droplet size and consequently increase the emulsified suspension viscosity.

3.2. Application of the Taylor model for the prediction of droplet size

The experimental data was analysed regarding the Taylor model of mechanical shearing. The droplet size fragmentation process depends mainly on the stresses applied on its surface during shearing. According to Eq. (1), the final droplet size R should be proportional to the ratio $Ca_{crit}\sigma/\eta_c\dot{\gamma}$. In the literature it was suggested that the viscosity of the continuous phase η_c has to be replaced by the effective viscosity of the emulsion (η_{eff}) in the case of highly concentrated emulsions.[17,20–22] Since for all conditions investigated no fracturing of the droplets was observed at a shear rate of $113\,s^{-1}$, the apparent viscosity of the HAPES measured at this shear rate was taken as η_{eff}.

It has been shown[13,20] that the viscosity ratio ($\rho = \eta_d/\eta_c$) between the dispersed (η_d) and continuous phase (η_c) greatly affects the ratio of the deforming viscous stress to the interfacial restoring stress which corresponds to the capillary number ($Ca = \eta_c\dot{\gamma}R_0/\sigma$). The stress ratio required for droplets breaking represents the critical capillary number, Ca_{crit}.

The correlation of Ca_{crit} with the viscosity ratio ρ presented by Grace[23] assumes simple shear conditions and is valid for any viscosity ratio ρ from 10^{-6} to 3.5. Based on this correlation the critical capillary number (Ca_{crit}) could be calculated with the viscosities of the alkane phase ($\eta_d = 0.92 \times 10^{-3}$ Pa s at 20 °C) and the HAPES ($\eta_c = \eta_{eff}$) resulting in viscosity ratios ρ between 4.6×10^{-4} and 4.5×10^{-3}. The calculated values are included in Fig. 5 and later used for comparison with the experimental data in Fig. 6.

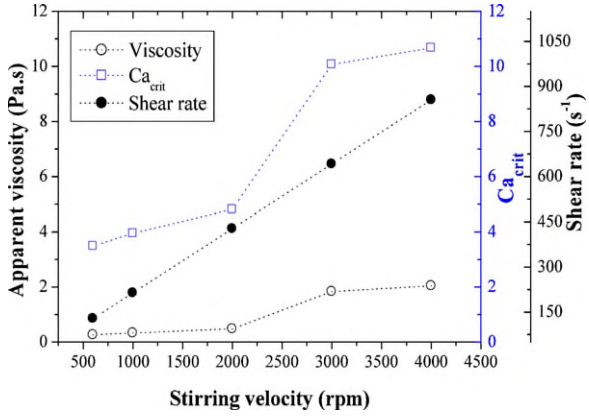

Fig. 5. Influence of emulsification stirring velocity on the shear rate, apparent viscosity and critical capillary number for HAPES containing 45 vol.% particle content.

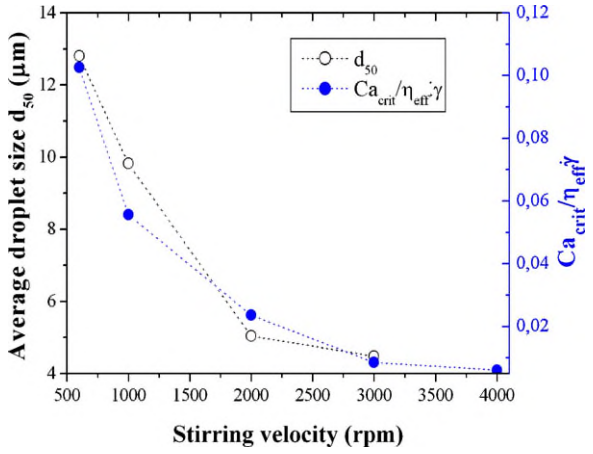

Fig. 6. Influence of emulsification stirring velocity on the average droplet size (d_{50}) experimentally measured and the ratio $Ca_{crit}/\eta_{eff}\dot{\gamma}$. Data analysis from HAPES containing 45 vol.% particle content suspensions emulsified from 600 to 4000 rpm.

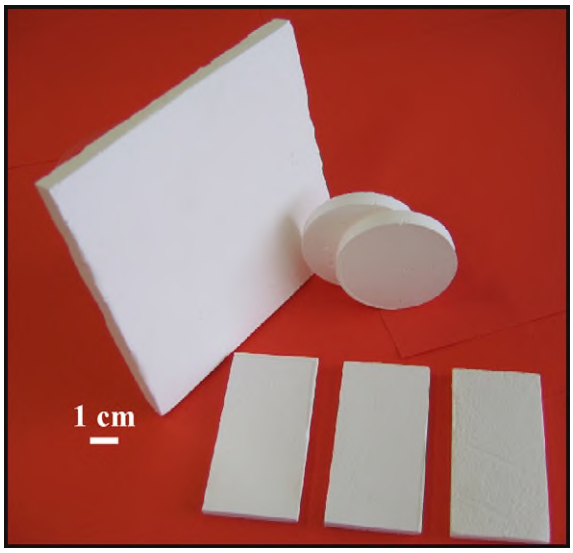

Fig. 7. Sintered ceramic foams with porosities beyond 70% produced by the presented direct foaming method.

The stirring velocity is directly proportional to the shear rate ($\dot{\gamma}$) applied on the droplets surface. The shear rate to which the highly concentrated emulsions are submitted could be approximated by $\dot{\gamma} = R_0\omega/(R_0 - R)$, where R_0 and R are the radius of the stirring container and of the mixing blade, respectively, and ω is the angular speed (rad s^{-1}) of the mixer.[22] The calculations were made considering that 1 rpm is 0.10471976 rad s^{-1}.

The influences of the emulsification stirring velocity on the shear rate, viscosity and Ca_{crit} of HAPES produced from 45 vol.% particle content suspensions are shown in Fig. 5. The shear rate applied to the system increases linearly with the stirring velocity. The HAPES viscosity rises with higher stirring velocities as the droplets concentration is increased restricting the mobility of the numerous small droplets. Ca_{crit} depends on the viscosity ratio ρ between decane and the emulsified suspension. The increase of the HAPES viscosity leads to a decrease in ρ and consequently to an increase of Ca_{crit}.

The experimental average droplet size (d_{50}) and the ratio $Ca_{crit}/\eta_{eff}\dot{\gamma}$ are plotted in Fig. 6 as a function of the stirring velocity. The results show a good agreement between the average droplet sizes from experimental data and the calculated data for the model. From this analysis, it can be concluded that the average droplet size decreases with increasing stirring velocity mainly as a result of the increase of the shear rate and consequently of the HAPES viscosity. These mechanical shearing effects are more significant than the increase of Ca_{crit} (as the increase of Ca_{crit} would contribute to the increase of the droplet size (Eq. (1))). It should be noted that the HAPES composition and in consequence the interfacial energy of the phases present in the system are kept constant for this analysis. However, this parameter exerts an important influence on the final droplet size as predicted in Eq. (1).

3.3. Ceramic foams

With the control of the studied parameters the droplet size distribution of the emulsified suspensions was efficiently tailored. However, for the realization of stable sintered ceramic foams, stable green bodies are first required. This means that no degradation of the wet foam during handling, drying and prepa-

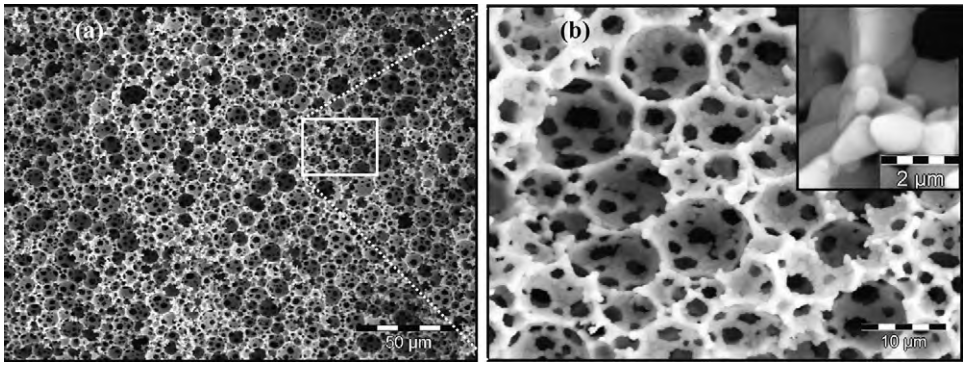

Fig. 8. Microstructure of sintered alumina foams (1550 °C/2 h) produced from HAPES containing 45 vol.% particle content emulsified under 2000 rpm. (a) Homogeneously distributed open porous cells and (b) detail of the interconnected cells with the inset showing a dense strut constituted by a monolayer of alumina particle.

ration for sintering occurs and phase separation, creaming or sedimentation and drainage effects are not allowed. Sufficient flexibility and plasticity have to be provided in order to exclude any crack formation. It can be stated that the transformation to the green bodies depends besides other factors on the viscosity of the HAPES and this is again influenced by the droplet concentration as well as by the particle content. The stability of the green bodies increases with the increase of the droplet concentration. However, if the emulsification velocity or the particle content in the suspensions is too high, the numerous small droplets are crowded together in a way that the restriction to their mobility leads to an abrupt increase of the viscosity (Fig. 4) resulting in a creaming effect. Furthermore, stable foams are favorably produced from sufficiently concentrated suspensions (minimum 30 vol.% alumina in this case).

The transition of HAPES to stable green bodies is achieved upon evaporation of the solvents with a minimal expansion of the pore formers. This simple process is continued by sintering (1550 °C, 2 h) and leads to strong ceramic foams with designed microstructural features, characterized by porosities up to 90% uniformly distributed throughout the sample with highly interconnected cells.

Sintered ceramic foams produced by this method are represented in Fig. 7. A typical sintered foam microstructure featuring interconnected cells with 3, 5 and 9 μm as d_{10}, d_{50} and d_{90}, respectively, is shown in Fig. 8. The dense struts composed of monolayers of alumina particles are represented in the detail.

4. Conclusions

The droplet size distribution in emulsified powder suspensions can be efficiently controlled by adjusting the parameters stirring velocity during the emulsification process and particle content of the alumina suspensions.

Considering the mechanical shearing processes the stresses applied to the emulsifying powder suspension can be used as expressed by the Taylor model to explain the rheological behaviour and the dispersion characteristics of the investigated HAPES systems.

Following these relations stable green bodies can be fabricated from highly concentrated suspensions without any organic binder while sedimentation, phase separation and crack formation are prevented. Emulsification limits are found at stirring velocities beyond 3000 rpm where critical concentrations of small sized droplets lead to creaming effects.

Cellular ceramics with open porosities up to 90% and cell sizes from 3 to 200 μm are prepared following the transition of HAPES to dried stable foams and subsequent sintering.

This process can also be extended to other oxide and non-oxide ceramics as well as to metallic powders. Taking into account the mechanical stability and microstructural features achieved by this process various applications of the cellular structures as filters, catalytic supports including supports for batteries, temperature control membranes and matrices for immobilized microorganisms are envisaged.

Acknowledgements

The authors would like to thank DFG for funding this project within the Research Group 1375 “Nonmetallic Porous Structures for Physical-Chemical Functions”. The help of Dr. S. Blindow (Bioceramics group, University of Bremen) concerning the fluorescence microscopy experiments is also gratefully appreciated.

References

1. Scheffler, M. and Colombo, P., ed., *Cellular Ceramics: Structure, Manufacturing, Properties and Applications*. Wiley-VCH, Weinheim, 2005.
2. Studart, A. R., Gonzenbach, U. T., Tervoort, E. and Gauckler, L. J., Processing routes to macroporous ceramics—a review. *J. Am. Ceram. Soc.*, 2006, **89**(6), 1771–1789.
3. Colombo, P., Conventional and novel processing methods for cellular ceramics. *Philos. Trans. Roy. Soc. A*, 2006, **364**(1838), 109–124.
4. Biasetto, L., Colombo, P., Innocentini, M. D. M. and Mullens, S., Gas permeability of microcellular ceramic foams. *Ind. Eng. Chem. Res.*, 2007, **46**, 3366–3372.
5. Gonzenbach, U. T., Studart, A. R., Steinlin, D., Tervoortand, E. and Gauckler, L. J., Processing of particle-stabilized wet foams into porous ceramics. *J. Am. Ceram. Soc.*, 2007, **90**(11), 3407–3414.
6. Garrn, I., Reetz, C., Brandes, N., Kroh, L. W. and Schubert, H., Clot-forming: the use of proteins as binder for producing ceramic foams. *J. Eur. Ceram. Soc.*, 2004, **24**, 579–587.
7. Barg, S., Soltmann, C., Pacheco, M., Koch, D. and Grathwohl, G., Cellular ceramics by direct foaming of ceramic powder suspensions. *J. Am. Ceram. Soc.*, 2008, **91**(9), 2823–2829.
8. Lavrentyeva, O. and Grathwohl, G., Zellularkeramik aus autarken Schäumungsprozessen keramischer Suspensionen. *Teil 1 Keram. Zeitschr.*, 2007, **2**, 88–93;
   Lavrentyeva, O. and Grathwohl, G., Zellularkeramik aus autarken Schäumungsprozessen keramischer Suspensionen. *Teil 2, Keram. Zeitschr.*, 2007, **4**, 260–265.
9. Hayati, I. N., Man, Y. B. C., Tan, C. P. and Aini, I. N., Stability and rheology of concentrated O/W emulsions based on soybean oil/palm kernel olein blends. *Food Res. Int.*, 2007, **40**, 1051–1061.
10. Imhof, A. and Pine, D. J., Ordered macroporous materials by emulsion templating. *Nature*, 1997, **389**, 948–951.
11. Akartuna, I., Studart, A. R., Tervoort, E. and Gauckler, L. J., Macroporous ceramics from particle-stabilized emulsions. *Adv. Mater.*, 2008, **20**, 4714–4718.
12. Akartuna, I., Studart, A. R., Tervoort, E., Urs, T., Gonzenbach, U. T. and Gauckler, L. J., Stabilization of oil-in-water emulsions by colloidal particles modified with short amphiphiles. *Langmuir*, 2008, **24**, 7161–7168.
13. Schramm, L. L., *Emulsions, Foams, and Suspensions: Fundamentals and Applications*. Wiley-VCH, Weinheim, 2006.
14. Mason, T. G. and Bibette, Emulsification in viscoelastic media. *Phys. Rev. Lett.*, 1996, **77**(16), 3481–3484.
15. Binks, B. P., Particles as surfactants similarities and differences. *Curr. Opin. Colloids Interf. Sci.*, 2002, **21**(7).
16. Taylor, G. I., The formation of emulsions in definable fields of flow. *Proc. Roy. Soc. Lond., Ser. A*, 1934, **146**(858), 501–523.
17. Gonzenbach, U. T., Studart, A. R., Tervoort, E. and Gauckler, L. J., Tailoring the microstructure of particle-stabilized wet foams. *Langmuir*, 2007, **23**(3), 1025–1032.
18. Mabille, C., Leal-Calderon, F., Bibette, J. and Schmitt, V., Monodisperse fragmentation in emulsions: mechanisms and kinetics. *Europhys. Lett.*, 2003, **61**, 708–714.
19. Schmitt, V., Leal-Calderon, F. and Bibette, J., Preparation of monodisperse particles and emulsions by controlled shear. *Top. Curr. Chem.*, 2003, **227**, 195–215.

20. Mason, T. G. and Bibette, Shearing rupturing of droplets in complex fluids. *Langmuir*, 1997, **13**, 4600–4613.
21. Welch, C. F., Rose, G. D., Malotky, D. and Eckersley, S. T., Rheology of high internal phase emulsions. *Langmuir*, 2006, **22**, 1544–1550.
22. Aronson, M. P., The role of free surfactant I destabilizing oil-in-water emulsions. *Langmuir*, 1989, **5**, 494–501.
23. Grace, H. P., Dispersion phenomena in high-viscosity immiscible fluid systems. *Chem. Eng. Commun.*, 1982, **14**(3–6), 225–277.